Scheme VII

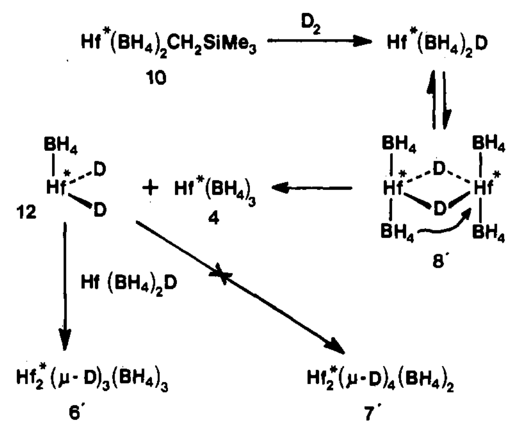

nonuclear bis(tetrahydroborate) complex **10** with D_2. By $^{31}P\{^1H\}$ NMR, the same distribution of **6** and **4** was obtained; however, the ^1H NMR spectrum indicated that **6** was fully deuterated in the bridging hydride positions (eq 5, Hf* = Hf[N(SiMe$_2$CH$_2$PMe$_2$)$_2$]). Unfortunately, we were unable to determine[43] if any deuterium incorporation had occurred on the BH_4^- ligands of either **6** or **4**.

$$\underset{\mathbf{10}}{Hf^*(BH_4)_2CH_2SiMe_3} \xrightarrow[4\ \text{atm}]{D_2} Hf^*{}_2(\mu\text{-}D)_3(BH_4)_3 + \underset{\mathbf{4}}{Hf^*(BH_4)_3} \quad (5)$$

This apparently specific incorporation of deuterium can be rationalized (Scheme VII) if the initially formed binuclear dideuteride **8′** undergoes BH_4^- migration (cf. Scheme II) to fragment into the mononuclear dideuteride **12** and the tris(tetrahydroborate) complex **4**. The fate of **12** is speculation, but the observed deuterium specifity for the production of **6** suggests a recombination process with the mononuclear precursor to **8′**, Hf*(BH$_4$)$_2$D (Hf* ≡ Hf[N(SiMe$_2$CH$_2$PMe$_2$)$_2$]). Simple dimerization of the intermediate **12** to generate **7′** (Scheme VII) can be excluded since none of this material is detected in any of these reactions.

The results of this deuteration experiment are also relevant to the pathway proposed for BH_4^- migration in **6** (Scheme III); the bridging deuterides of **6′** are clearly not involved in the process by which BH_4^- ligands are exchanged between hafnium centers since we observe no scrambling of hydrogen into the bridging positions from the BH_4^- groups as would be expected on the basis of the well-known[24] bridge to terminal B–H exchange process.

Conclusions

BH_3 cleavage from the mononuclear hafnium–tris(tetrahydroborate) complex **4** produces two new and unusual binuclear hydrides, **6** and **7**. The nonrigid behavior of these derivatives can be rationalized by invoking a novel intramolecular, intermetal BH_4^- migration in **6**, while for **7**, a "rotation" of the ends of the dimer satisfactorily explains the observed spectroscopic data.

The mechanism of formation of the binuclear complex **6** from the mononuclear precursor **4** has been probed by product analysis and deuteration studies. A simple, stepwise removal of BH_3 is not involved, but rather, a fragmentation–recombination process is likely to be operative.

It is significant that this ancillary ligand system promotes the formation of binuclear complexes which do not have analogues to derivatives that incorporate cyclopentadienyl type ligands. In particular, a binuclear zirconium complex,[39] which contains the $C_5Me_5^-$ ancillary ligand, adopts completely different types of binding modes for the hydride ligands than is found in the isoelectronic binuclear tetrahydride **7**, which is stabilized by the tridentate ligand $^-N(SiMe_2CH_2PMe_2)_2$. Further work on this type of ancillary ligand system coordinated to the early transition metals is in progress.

Acknowledgment. This work was supported by the Natural Sciences and Engineering Research Council of Canada. Thanks are due to Professor James Trotter for the use of his X-ray diffractometer and crystal structure solving programs.

Note Added in Proof. After submission of this manuscript, a paper by Bergman et al. reported the X-ray crystal structure of a bridging BH_4^- analogous to that proposed by us in Scheme III: Gilbert, T. M.; Hollander, F. J.; Bergman, R. G. *J. Am. Chem. Soc.* **1985**, *107*, 3508.

Registry No. **4**, 83634-66-6; **5**, 98720-53-7; **6**, 98720-54-8; **7**, 98720-55-9; **9**, 98720-56-0; **10**, 98720-57-1; **11**, 98720-58-2; HfCl$_3$[N(SiMe$_2$CH$_2$PMe$_2$)$_2$], 98758-74-8; HfCl$_3$[N(SiMe$_2$CH$_2$P(*i*-Pr)$_2$)$_2$], 94372-16-4; PMe$_3$, 594-09-2; NMe$_3$, 75-50-3.

Supplementary Material Available: Calculated coordinates and isotropic thermal parameters for the "organic" hydrogen atoms (Table VI), anisotropic thermal parameters (Table VII), torsion angles (Table VIII), a stereoview of refined borohydride H atom positions, and measured and calculated structure factor amplitudes (Table IX) (52 pages). Ordering information is given on any current masthead page.

---

[43] Both IR and ^2H NMR analyses were attempted, but no conclusive results were obtained.

[44] In this paper the periodic group notation is in accord with recent actions by IUPAC and ACS nomenclature committees. A and B notation is eliminated because of wide confusion. Groups IA and IIA become groups 1 and 2. The d-transition elements comprise groups 3 through 12, and the p-block elements comprise groups 13 through 18. (Note that the former Roman number designation is preserved in the last digit of the new numbering: e.g., III → 3 and 13.)

Contribution from the Departments of Chemistry, University of Southern California, Los Angeles, California 90089-1062, and University of Notre Dame, Notre Dame, Indiana 46556

Coordinated Hexafluoroantimonate: X-ray Crystal Structure of the Intermediate-Spin Iron(III) Tetraphenylporphinato Complex Fe(TPP)(FSbF$_5$)·C$_6$H$_5$F

KENNETH SHELLY,[1] T. BARTCZAK,[2] W. ROBERT SCHEIDT,*[2] and CHRISTOPHER A. REED*[1]

Received May 30, 1985

In order to resolve inconsistencies in the literature concerning the spin state and structure of Fe^{III}(TPP)(SbF$_6$) the X-ray crystal structure of (hexafluoroantimonato)(*meso*-tetraphenylporphinato)iron(III)–fluorobenzene, Fe(TPP)(FSbF$_5$)·C$_6$H$_5$F, has been determined. Crystal data: orthorhombic, space group $Pna2_1$, $Z = 4$, $a = 25.754$ (6) Å, $b = 10.748$ (2) Å, $c = 15.707$ (4) Å, $\rho_{calcd} = 1.528$ g/cm^3, $\rho_{obsd} = 1.54$ g/cm^3. Diffraction data were collected by the θ–2θ scan method; all unique data to $2\theta \leq 66.8°$ were measured. A total of 6126 reflections were used in the structure determination; final discrepancy indices are $R_1 = 0.049$ and $R_2 = 0.057$. The complex is not ionic. The hexafluoroantimonate ligand is found to coordinate to iron in a monodentate fashion with an FeFSb bridge angle of 150.4 (2)° and an Fe–F bond length of 2.105 (3) Å. The short average Fe–N distance (1.978 (3) Å) and the small out-of-plane iron atom displacement are in accord with a nearly pure $S = {}^3/_2$ spin state.

The perchlorato complex Fe(OClO$_3$)(TPP)[3,4] is representative of a number of iron(III) porphyrins that have weak-field axial ligation.[5-12] A common feature of such complexes is their unusual admixed intermediate $S = {}^3/_2, {}^5/_2$ spin states, which give rise to

0020-1669/85/1324-4325$01.50/0 © 1985 American Chemical Society

magnetic moments that can be considerably depressed below the 5.9 μ_B value of the $S = {}^5/_2$ high-spin state. The mixing of $S = {}^3/_2$ character into the spin state is recognized to arise from increasing the tetragonality of the ligand field.[13,14] In principle, the production of a pure $S = {}^3/_2$ intermediate-spin state is straightforward. If an iron(III) heme could be produced devoid of axial ligation, e.g. $[Fe(TPP)]^+$, the resulting tetragonal ligand field would cause one d orbital ($d_{x^2-y^2}$, whose lobes are directed at the porphinato nitrogen atoms) to be very much higher in energy than the other four. This orbital would then remain unoccupied in a d^5 configuration and a pure $S = {}^3/_2$ spin state would result. A magnetic moment approaching the spin-only value of 3.9 μ_B would be expected.

However, the synthesis of a bare cationic porphyrin complex such as $[Fe(TPP)]^+$ is not a trivial task. Axial ligation by donor solvents may thwart attempts to synthesize such a complex in solvents that might be best suited for ion separation.[10,11,15] In nondonor solvents such as benzene or dichloromethane a more severe problem is preventing coordination of the counterion. The short Fe–O bond of 2.03 Å to the coordinated perchlorate in $Fe(OClO_3)(TPP)$ illustrates the strong desire of the hypothetical unligated $[Fe(TPP)]^+$ to attain electroneutrality. Indeed, with a variety of the typical noncoordinating anions of aqueous chemistry such as PF_6^-, BF_4^-, SbF_6^-, and $CF_3SO_3^-$ we had earlier concluded that the bare $[Fe(TPP)]^+$ cation was synthetically unattainable.[3] With tetraphenylborate as counterion a neutral phenyl complex results from boron–phenyl bond cleavage.[3,16] With tricyanomethanide as counterion symmetrical weak axial interactions with the cyano nitrogen atoms are observed with Fe–N = 2.32 Å.[9] These studies highlight a quite general problem of coordination chemistry; namely, there is probably no such thing as a truly noncoordinating anion.

The particular case of SbF_6^- as counterion for $[Fe(TPP)]^+$ has been explored by several groups.[3,17,18] In our original synthesis[3] of $Fe(TPP)(SbF_6)$ we concluded that the hexafluoroantimonate was coordinated to the iron atom. This was based on its benzene solubility and the asymmetric broadening of the infrared absorption of SbF_6 at 660 cm^{-1}. Subsequently, Baldwin et al.[17] formulated the nonsolvated material as an ionic compound containing the square-planar ferric ion, $[Fe(TPP)][SbF_6]$. This was based on its room-temperature magnetic moment of 4.27 μ_B, which approaches that expected for a pure $S = {}^3/_2$ spin state. Later, Quinn et al.[18] prepared this compound for subsequent axial ligation studies. Its EPR spectrum was reported to show a mixture of high- and intermediate-spin species in frozen toluene solution with the latter species dominant.

Because of the difficulties in reconciling all of this literature and because of the resistance of this compound to give a reliable elemental analysis,[3,17,19] the true nature and structure of $Fe(TPP)(SbF_6)$ has remained unclear. This, along with our belief that at present no "noncoordinating" anion exists with respect to $[Fe(TPP)]^+$, has prompted us to determine the X-ray crystal structure of the hexafluoroantimonate of iron(III) tetraphenylporphinate.

Experimental Section

General Procedures. Moisture was rigorously excluded from the reagents and solvents used in the preparation of $Fe(TPP)(FSbF_5)$ by using a Vacuum Atmospheres Corp. glovebox under a He atmosphere. Infrared specra, as KBr disks, were recorded on a Perkin-Elmer (Model 281) spectrophotometer. Visible spectra were obtained on a Hewlett-Packard 8450A spectrophotometer. Spectral samples were prepared in the drybox and protected from moisture when brought out into air.

Materials. Silver hexafluoroantimonate (Ozark-Mahoning) was vacuum-dried overnight. Solvents were purified by stirring with H_2SO_4 (ca. 3 h), washing with water until neutral, predrying with $CaSO_4$ (24 h), and degassing with N_2. Solvents were distilled inside the drybox from CaH_2 (hexane, fluorobenzene) or sodium/benzophenone (toluene). Alumina was prepared by making a slurry of neutral or basic alumina with 10% aqueous HBr, filtering, and drying.

Fe(TPP)Cl was prepared by a literature method.[20] This was converted to the bromide by washing a dichloromethane solution with aqueous NH_4OH (to form $[Fe(TPP)]_2O$), and then washing with aqueous HBr. The CH_2Cl_2 layer was separated and refluxed with 2,3-dichloro-5,6-dicyanobenzoquinone (ca. 10 mg) for 20 min to oxidize any chlorin that had formed. This solution was chromatographed on a column of acidic (HBr) aluminia,[21] with CH_2Cl_2 as eluent. The eluent was concentrated, and addition of dry methanol produced crystalline Fe(TPP)Br.

$Fe(TPP)(FSbF_5)\cdot C_6H_5F$. Fe(TPP)Br (262 mg, 0.35 mmol) was stirred in refluxing fluorobenzene (10 mL). Solid $AgSbF_6$ (135 mg, 0.39 mmol) was added and the mixture refluxed for 30 min to ensure complete reaction. The resulting solution was filtered through a fine fritted funnel to remove AgBr. Hexane diffusion into the filtrate (5 days) yielded purple crystals, some of which were suitable for X-ray studies. The total yield of $Fe(TPP)(FSbF_5)\cdot C_6H_5F$ was 255 mg (73%). The infrared spectrum contains a broad asymmetric absorption due to SbF_6^- at 660 cm^{-1}.

X-ray Structure Determination. Preliminary examination of a crystal with dimensions of 0.55 × 0.60 × 0.95 mm established a four-molecule unit cell with possible space groups $Pna2_1$ or $Pnma$. The noncentrosymmetric space group $Pna2_1$ was used to solve the structure. This choice was fully confirmed by all subsequent developments during structure solution and refinement. Intensity data and final cell constants were measured with a Nicolet P1 automatic diffractometer. All measurements were made with use of graphite-monochromated Mo Kα radiation (λ = 0.71073 Å). Least-squares refinement of the setting angles of 30 reflections with $2\theta > 25.1°$ led to the cell constants a = 25.754 (6) Å, b = 10.748 (2) Å, and c = 15.707 (4) Å. For a cell content of $[Fe(TPP)(FSbF_5)]\cdot C_6H_5F$ and Z = 4, the calculated density was 1.528 g/cm^3; the experimental density was 1.54 g/cm^3.

Intensity data were measured with use of graphite-monochromated Mo Kα radiation and θ–2θ scans; the scan rate was chosen after a prescan of each reflection. Four standard reflections were measured after every fifty reflections to monitor the stability of the crystal. No decline in the intensities of the standard reflections was observed. An empirical absorption correction was applied (μ_B = 1.03 mm^{-1}, Mo Kα). A total of 6126 reflections having $(\sin\theta)/\lambda < 0.774$ Å^{-1} and $F_o > 3\sigma(F_o)$ were retained as observed after correction for Lorentz, polarization, and absorption effects (73% of the theoretical number possible). These data were used in the solution and refinement of the structure.

The structure was solved in the space group $Pna2_1$ by the heavy-atom method.[22] The Patterson map was used to obtain the coordinates of the

---

(1) University of Southern California.

(2) University of Notre Dame.

(3) Reed, C. A.; Mashiko, T.; Bentley, S. P.; Kastner, M. E.; Scheidt, W. R.; Spartalian, K.; Lang, G. *J. Am. Chem. Soc.* **1979**, *101*, 2948–2958.

(4) Abbreviations used in this paper: TPP = *meso*-tetraphenylporphinate; OEP = octaethylporphinate; 3-Cl-py = 3-chloropyridine.

(5) Dolphin, D. H.; Sams, J. R.; Tsin, T. B. *Inorg. Chem.* **1977**, *16*, 711–713.

(6) Masuda, H.; Taga, T.; Osaki, K.; Sugimoto, H.; Yoshida, Z.-I.; Ogoshi, H. *Inorg. Chem.* **1980**, *19*, 950–955.

(7) Goff, H.; Shimomura, E. *J. Am. Chem.* Soc. **1980**, *102*, 31–37.

(8) Boersma, A. D.; Goff, H. M. *Inorg. Chem.* **1982**, *21*, 581–586.

(9) Summerville, D. A.; Cohen, I. A.; Hatano, K.; Scheidt, W. R. *Inorg. Chem.* **1978**, *17*, 2906–2910.

(10) Masuda, H.; Taga, T.; Osaki, K.; Sugimoto, H.; Yoshida, Z.; Ogoshi, H. *Bull. Chem. Soc. Jpn.* **1982**, *55*, 3891–3895.

(11) Behere, D. V.; Birdy, R.; Mitra, S. *Inorg. Chem.* **1984**, *23*, 1978–1981.

(12) Scheidt, W. R.; Geiger, D. K.; Hayes, R. G.; Lang, G. *J.Am. Chem. Soc.* **1983**, *105*, 2625–2632.

(13) Maltempo, M. M. *Q. Rev. Biophys.* **1976**, *9*, 181–215.

(14) Scheidt, W. R.; Reed, C. A. *Chem. Rev.* **1981**, *81*, 543–555.

(15) Mashiko, T.; Kastner, M. E.; Spartalian, K.; Scheidt, W. R.; Reed, C. A. *J. Am. Chem. Soc.* **1978**, *100*, 6354–6362.

(16) Doppelt, P. *Inorg. Chem.* **1984**, *23*, 4009–4011.

(17) Baldwin, J. E.; Haraldsson, G. G.; Jones, J. G. *Inorg. Chim. Acta* **1981**, *51*, 29–33.

(18) Quinn, R.; Nappa, M.; Valentine, J. S. *J. Am. Chem. Soc.* **1982**, *104*, 2588–2595.

(19) Repeated attempts by us at elemental analyses, even with X-ray-quality crystals, have given unsatisfactory results. We suppose the problem lies, at least in part, with interference by antimony.

(20) Fleischer, E. B.; Palmer, J. M.; Srivastava, T. S.; Chatterjee, A. *J. Am. Chem. Soc.* **1971**, *93*, 3162–3167.

(21) We have found that chromatographing Fe(TPP)Br with commercial acidic alumina (which is presumably acidified with HCl) results in a product that is predominantly Fe(TPP)Cl.

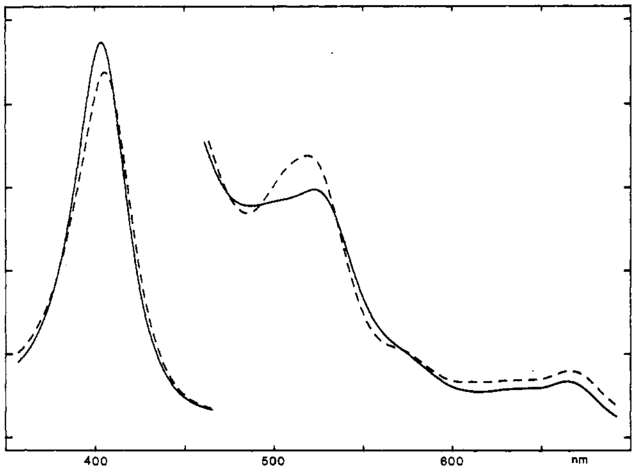

Figure 1. Visible spectra of Fe(TPP)(FSbF$_5$) in toluene solution. The solid line is a sample made up in a drybox (λ_{max} 403, 523, 664 nm). The dotted line is the same sample after brief exposure to air (λ_{max} 406, 518, 572 sh, 667 nm).

iron and antimony atoms; three cycles of difference Fourier syntheses served to find all remaining atoms. After several cycles of full-matrix least-squares refinement, the question of the correct hand of the molecule in the polar space group was examined. Further refinement with the arbitrarily chosen hand was continued after the inclusion of $\Delta f''$ terms for both iron and antimony. A second path, with the opposite hand, was also begun. Both alternatives were taken to convergence with anisotropic temperature factors for all atoms. In both cases, the *z* coordinate of the antimony atom was held constant to fix the origin of the space group. The first choice converged at $R_1 = 0.054$ and $R_2 = 0.063$. The alternate choice converged at $R_1 = 0.056$ and $R_2 = 0.066$. The first choice is clearly the correct enantiomorph and is reported herein. As would be expected, there is a larger spread in the values of the chemically equivalent bond distances for the incorrect enantiomorph, especially those involving the antimony and iron atoms. The average Sb–F distances (uncoordinated fluorides) are 1.836 (32) and 1.836 (24) Å, for the incorrect and correct enantiomorphs, respectively, where the values in parentheses are the calculated variances. The range of values is 1.799–1.898 and 1.809–1.871 Å, respectively. The values of the corresponding Fe–N distances are 1.979 (24) and 1.981 (3) Å, and the ranges are 1.952–2.005 and 1.979–1.983 Å, respectively. At this point a difference Fourier gave evidence of the position of many hydrogen atoms. All hydrogen atoms were included in subsequent cycles of least-squares refinement as fixed idealized contributors (C–H = 0.95 Å, B(H) = B(C) + 1.0 Å^2). The high temperature factor of the fluorine atom of the fluorobenzene solvate molecule and some small residual densities near other carbon atoms of the solvate suggest some possible orientational disorder of the solvent molecule. Final cycles of full-matrix least-squares refinement were carried to convergence with anisotropic temperature factors for all heavy atoms. The final discrepancy indices were $R_1 = 0.049$ and $R_2 = 0.057$[23] with an error of fit of 1.64. There were no significant features on the final electron density difference map; the highest peak was 0.85 e/Å^3 at a position near the Sb atom. Final atomic coordinates are listed in Table I. Tables A and B, tables of anisotropic temperature factors and the fixed hydrogen atom coordinates, are available as supplementary material.

Results and Discussion

Properties. Fe(TPP)(FSbF$_5$) can be cleanly synthesized by the silver salt metathesis method[3] in aromatic solvents such as benzene, toluene, or fluorobenzene as long as particular care is taken to exclude moisture. Both the solid and its solutions are moisture sensitive.

Table I. Fractional Atomic Coordinates for [Fe(TPP)(FSbF$_5$)]·C$_6$H$_5$F[a]

atom	*x*	*y*	*z*
Sb	0.214088 (13)	0.218207 (28)	0.5000
Fe	0.127084 (23)	−0.05714 (5)	0.57120 (5)
N(1)	0.17238 (15)	−0.0613 (4)	0.67280 (27)
N(2)	0.08594 (14)	0.0777 (3)	0.62369 (27)
N(3)	0.07573 (13)	−0.0681 (3)	0.47769 (24)
N(4)	0.16201 (15)	−0.2082 (3)	0.52692 (27)
C(a1)	0.21116 (19)	−0.1441 (5)	0.6901 (4)
C(a2)	0.17175 (20)	0.0189 (5)	0.7411 (3)
C(a3)	0.09744 (18)	0.1448 (4)	0.6972 (3)
C(a4)	0.04352 (17)	0.1372 (4)	0.5896 (3)
C(a5)	0.03558 (17)	0.0128 (5)	0.4618 (3)
C(a6)	0.07553 (17)	−0.1501 (5)	0.4094 (3)
C(a7)	0.15038 (19)	−0.2726 (4)	0.4539 (4)
C(a8)	0.20426 (19)	−0.2677 (5)	0.5622 (4)
C(b1)	0.23282 (27)	−0.1164 (6)	0.7712 (4)
C(b2)	0.20856 (23)	−0.0165 (6)	0.8024 (4)
C(b3)	0.06204 (21)	0.2454 (5)	0.7079 (4)
C(b4)	0.02913 (21)	0.2400 (5)	0.6430 (4)
C(b5)	0.01119 (21)	−0.0185 (6)	0.3826 (4)
C(b6)	0.03622 (20)	−0.1182 (5)	0.3509 (4)
C(b7)	0.18603 (22)	−0.3740 (5)	0.4439 (5)
C(b8)	0.21912 (21)	−0.3688 (5)	0.5088 (6)
C(m1)	0.13842 (20)	0.1196 (5)	0.7522 (3)
C(m2)	0.01939 (17)	0.1096 (4)	0.5128 (4)
C(m3)	0.10909 (20)	−0.2500 (5)	0.3983 (3)
C(m4)	0.22789 (21)	−0.2402 (5)	0.6377 (4)
C(1)	0.14888 (24)	0.2070 (5)	0.8250 (4)
C(2)	0.1209 (3)	0.2031 (9)	0.8983 (5)
C(3)	0.1340 (4)	0.2801 (10)	0.9657 (5)
C(4)	0.1731 (4)	0.3635 (8)	0.9582 (6)
C(5)	0.1988 (3)	0.3707 (7)	0.8849 (6)
C(6)	0.1880 (3)	0.2913 (6)	0.8189 (5)
C(7)	−0.02763 (20)	0.1842 (5)	0.4873 (4)
C(8)	−0.07583 (22)	0.1384 (7)	0.5001 (8)
C(9)	−0.11765 (27)	0.2167 (11)	0.4730 (8)
C(10)	−0.1092 (5)	0.3306 (11)	0.4400 (7)
C(11)	−0.0617 (3)	0.3733 (8)	0.4279 (6)
C(12)	−0.02200 (28)	0.3011 (6)	0.4505 (5)
C(13)	0.10088 (20)	−0.3340 (5)	0.3232 (3)
C(14)	0.1357 (3)	−0.3337 (7)	0.2558 (5)
C(15)	0.1260 (4)	−0.4101 (8)	0.1845 (5)
C(16)	0.0826 (3)	−0.4869 (7)	0.1837 (5)
C(17)	0.05087 (27)	−0.4894 (7)	0.2501 (5)
C(18)	0.05894 (24)	−0.4110 (6)	0.3194 (4)
C(19)	0.27424 (23)	−0.3176 (6)	0.6667 (5)
C(20)	0.32108 (26)	−0.2659 (7)	0.6813 (5)
C(21)	0.3623 (3)	−0.3420 (13)	0.7086 (7)
C(22)	0.3521 (4)	−0.4677 (11)	0.7242 (8)
C(23)	0.3078 (4)	−0.5139 (12)	0.7091 (14)
C(24)	0.2690 (4)	−0.4397 (8)	0.6809 (9)
Fe(1)	0.17406 (11)	0.06931 (26)	0.50378 (27)
F(2)	0.25566 (19)	0.3607 (3)	0.4948 (5)
F(3)	0.17663 (26)	0.2830 (5)	0.5877 (4)
F(4)	0.25857 (27)	0.1430 (7)	0.5756 (6)
F(5)	0.25235 (26)	0.1466 (4)	0.4137 (5)
F(6)	0.17000 (28)	0.2857 (5)	0.4219 (5)
C(25)	0.0341 (6)	0.7671 (18)	0.6573 (15)
C(26)	0.0687 (6)	0.7460 (13)	0.7093 (10)
C(27)	0.1001 (5)	0.6480 (16)	0.7024 (8)
C(28)	0.0926 (6)	0.5595 (10)	0.6383 (10)
C(29)	0.0611 (7)	0.5766 (19)	0.5867 (8)
C(30)	0.0279 (7)	0.674 (4)	0.5894 (18)
F(7)	−0.0050 (8)	0.7051 (29)	0.5471 (16)

[a] The estimated standard deviations of the least significant digits are given in parentheses.

The visible spectrum of Fe(TPP)(FSbF$_5$) in toluene solution is shown as the solid line in Figure 1. It is virtually identical in benzene or fluorobenzene but is clearly different from that which has appeared in the literature,[17,18] However, brief exposure of the spectral solution to atmospheric moisture or anaerobic water reproduces the published spectrum (dashed line). A possible explanation is the formation of an aquated species such as Fe(FSbF$_5$)(H$_2$O)(TPP) or [Fe(TPP)(OH$_2$)$_2$]$^+$SbF$_6^-$. Prolonged exposure of solutions to moisture causes eventual hydrolysis to Fe(TPP)F[24] as judged by the maxima in the α,β region.

---

(22) Programs used in this study included local modifications of Jacobson's ALLS and ALFF, Busing and Levy's ORFFE and ORFLS, Zalkin's FORDAP, and Johnson's ORTEP2. Atomic form factors were from: Cromer, D. T.; Mann, J. B. *Acta Crystallogr., Sect. A: Cryst. Phys., Diffr., Theor. Gen. Crystallogr.* **1968**, *A24*, 321–323. Real and imaginary corrections for anomalous dispersion in the form factors of the iron and antimony atoms were from: Cromer, D. T.; Liberman, D. J. *J. Chem. Phys.* **1970**, *53*, 1891–1898. Scattering factors for hydrogen were from: Stewart, R. F.; Davidson, E. R.; Simpson, W. T. *Ibid.* **1965**, *42*, 3175–3187.

(23) $R_1 = \sum||F_o| - |F_c||/\sum|F_o|$ and $R_2 = [\sum w(|F_o| - |F_c|)^2/\sum w(F_o)^2]^{1/2}$.

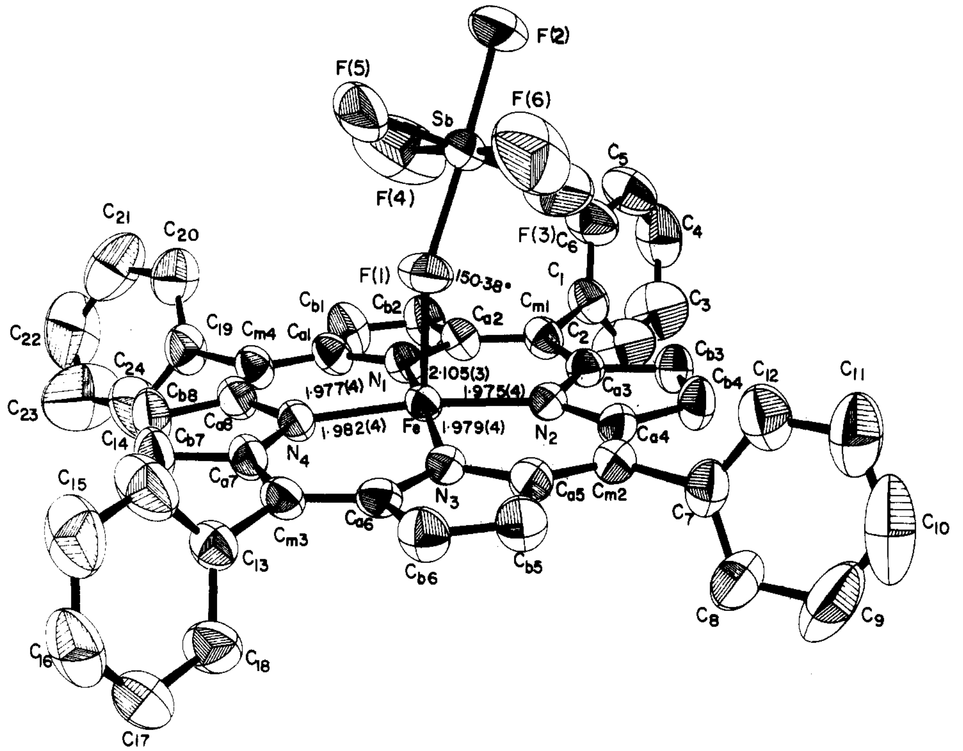

Figure 2. Computer-drawn model of the Fe(TPP)(FSbF$_5$) molecule. The labeling scheme for the atoms is shown. Bond distances in the coordination group are shown. Ellipsolids are contoured to enclose 50% of the electron density.

The EPR spectrum in toluene at 11 K consists of two broad signals with $g_{\parallel} = 2.0$ and $g_{\perp} \simeq 4.5$. A $g_{\perp} \simeq 6$ signal, typical of high-spin ferric hemes, is not observed except for the hint of a shoulder on the low-field side of the $g = 4.5$ band. The magnetic moment in the solid state at 300 K is 4.14 μ_B (corrected for diamagnetism). This is consistent with an almost pure $S = {}^3/_2$ intermediate-spin state. Complete details of the magnetic properties of Fe(TPP)(FSbF$_5$) will be presented elsewhere along with those of other closely related species.[25]

Structure. The structure of the Fe(TPP)(FSbF$_5$) molecule is shown in Figure 2. It illustrates the most significant feature of the structure—a coordinated SbF$_6^-$ anion. This is in agreement with our original expectation[3] but contrasts with the suggestion of an ionic formulation by Baldwin et al.[17] The possibility that a different crystalline form could be ionic seems to us rather remote. The hexafluoroantimonate ion binds to the iron through an Fe–F–Sb bridge bond with Fe–F = 2.105 (3) Å and an FeFSb angle of 150.4 (2)°. The Fe–F bond vector is tipped by about 3° from the heme normal. Although hexafluoroantimonate is not a common ligand, it has previously been observed as a weakly bonding ligand to some coordinatively unsaturated cations.[26] The average value[27] of the five noncoordinated Sb–F bond distances is 1.906 (23) Å (corrected for thermal motion) or 1.839 (20) Å (uncorrected) and is quite comparable to the 1.903 (6) Å value observed for NS$^+$SbF$_6^-$ (corrected for thermal motion)[28] or the 1.844 (5) Å value observed in K$^+$SbF$_6^-$ (uncorrected for thermal motion).[29] The Sb–F distance involving the bridging fluorine is 1.905 (3) Å, somewhat shorter than the bridging Sb–F distance (2.030 (4) Å) in the Sb$_2$F$_{11}^-$ anion.[28] This observation suggests rather weak bonding between the iron and the bridging fluorine

Table II. Bond Lengths (Å) in [Fe(TPP)(FSbF$_5$)]·C$_6$H$_5$F[a]

Fe–N(1)	1.977 (4)	C(1)–C(2)	1.360 (10)
Fe–N(2)	1.975 (4)	C(1)–C(6)	1.360 (10)
Fe–N(3)	1.979 (4)	C(2)–C(3)	1.385 (12)
Fe–N(4)	1.982 (4)	C(3)–C(4)	1.356 (13)
Fe–F(1)	2.105 (3)	C(4)–C(5)	1.330 (13)
N(1)–C(a1)	1.365 (7)	C(5)–C(6)	1.371 (11)
N(1)–C(a2)	1.376 (7)	C(7)–C(8)	1.351 (9)
N(2)–C(a3)	1.393 (6)	C(7)–C(12)	1.391 (10)
N(2)–C(a4)	1.375 (6)	C(8)–C(9)	1.433 (12)
N(3)–C(a5)	1.374 (6)	C(9)–C(10)	1.348 (17)
N(3)–C(a6)	1.388 (6)	C(10)–C(11)	1.325 (16)
N(4)–C(a7)	1.373 (7)	C(11)–C(12)	1.331 (11)
N(4)–C(a8)	1.378 (7)	C(13)–C(14)	1.388 (10)
C(a1)–C(m4)	1.389 (8)	C(13)–C(18)	1.364 (9)
C(a1)–C(b1)	1.421 (9)	C(14)–C(15)	1.412 (11)
C(a2)–C(b2)	1.405 (8)	C(15)–C(16)	1.393 (12)
C(a2)–C(m1)	1.393 (8)	C(16)–C(17)	1.325 (11)
C(a3)–C(b3)	1.424 (7)	C(17)–C(18)	1.393 (10)
C(a3)–C(m1)	1.390 (8)	C(19)–C(20)	1.348 (10)
C(a4)–C(b4)	1.436 (8)	C(19)–C(24)	1.340 (11)
C(a4)–C(m2)	1.389 (8)	C(20)–C(21)	1.411 (12)
C(a5)–C(b5)	1.432 (8)	C(21)–C(22)	1.396 (18)
C(a5)–C(m2)	1.378 (8)	C(22)–C(23)	1.268 (17)
C(a6)–C(b6)	1.410 (8)	C(23)–C(24)	1.354 (13)
C(a6)–C(m3)	1.390 (8)	Sb–F(1)	1.905 (3)
C(a7)–C(b7)	1.433 (7)	Sb–F(2)[b]	1.923 (4)
C(a7)–C(m3)	1.397 (8)	Sb–F(3)[b]	1.877 (5)
C(a8)–C(b8)	1.425 (9)	Sb–F(4)[b]	1.929 (7)
C(a8)–C(m4)	1.365 (9)	Sb–F(5)[b]	1.915 (5)
C(b1)–C(b2)	1.335 (10)	Sb–F(6)[b]	1.888 (7)
C(b3)–C(b4)	1.327 (9)	C(25)–C(26)	1.23 (2)
C(b5)–C(b6)	1.346 (8)	C(25)–C(30)	1.46 (5)
C(b7)–C(b8)	1.330 (11)	C(26)–C(27)	1.34 (2)
C(m1)–C(1)	1.505 (8)	C(27)–C(28)	1.40 (2)
C(m2)–C(7)	1.506 (7)	C(28)–C(29)	1.16 (2)
C(m3)–C(13)	1.501 (8)	C(29)–C(30)	1.35 (4)
C(m4)–C(19)	1.524 (8)	C(30)–F(7)	1.12 (2)

[a] The numbers in parentheses are the estimated standard deviations.
[b] The bond lengths are corrected for thermal motion. The fluorine atoms are assumed to ride on the Sb atom.

---

(24) Anzai, K.; Hatano, K.; Lee, Y. J.; Scheidt, W. R. *Inorg. Chem.* **1981**, *20*, 2337–2339.

(25) Shelly, K.; Reed, C. A.; Scheidt, W. R., manuscript in preparation.

(26) Edwards, A. J.; Khallow, K. I. *J. Chem. Soc., Chem. Commun.* **1984**, 50–51. Fawcett, J.; Holloway, J. H.; Laycock, D.; Russel, D. R. *J. Chem. Soc., Dalton Trans.* **1982**, 1355–1360.

(27) The number in parentheses following an average value is the estimated standard deviation calculated on the basis that all values are drawn from the same population.

(28) Clegg, W.; Glemser, O.; Harms, K.; Hartmann, G.; Mews, R.; Noltmeyer, M.; Sheldrick, G. *Acta Crystallogr., Sect. B: Struct. Crystallogr. Cryst. Chem.* **1981**, *B37*, 548–552.

(29) Kruger, G. J.; Pistorius, C. W. F. T.; Heynes, A. M. *Acta Crystallogr., Sect. B: Struct. Crystallogr. Cryst. Chem.* **1976**, *B32*, 2916–2918.

Table III. Bond Angles (deg) in [Fe(TPP)(FSbF$_5$)]·C$_6$H$_5$F[a]

N(1)FeN(2)	89.78 (17)	N(3)C(a6)C(b6)	110.61 (45)
N(1)FeN(3)	172.51 (17)	N(3)C(a6)C(m3)	125.80 (47)
N(1)FeN(4)	89.82 (17)	C(b6)C(a6)C(m3)	123.59 (48)
N(1)FeF(1)	94.69 (17)	N(4)C(a7)C(b7)	109.58 (48)
N(2)FeN(3)	89.73 (16)	N(4)C(a7)C(m3)	126.89 (46)
N(2)FeN(4)	172.17 (17)	C(b7)C(a7)C(m3)	123.46 (50)
N(2)FeF(1)	92.56 (15)	N(4)C(a8)C(b8)	109.25 (53)
N(3)FeN(4)	89.64 (16)	N(4)C(a8)C(m4)	126.89 (50)
N(3)FeF(1)	92.81 (16)	C(b8)C(a8)C(m4)	123.81 (54)
N(4)FeF(1)	95.27 (15)	C(a1)C(b1)C(b2)	108.32 (55)
FeN(1)C(a1)	127.41 (37)	C(a2)C(b2)C(b1)	106.36 (57)
FeN(1)C(a2)	127.42 (35)	C(a3)C(b3)C(b4)	106.50 (48)
C(a1)N(1)C(a2)	105.17 (44)	C(a4)C(b4)C(b3)	108.54 (48)
FeN(2)C(a3)	127.73 (33)	C(a5)C(b5)C(b6)	107.40 (49)
FeN(2)C(a4)	127.24 (35)	C(a6)C(b6)C(b5)	107.19 (51)
C(a3)N(2)C(a4)	104.50 (40)	C(a7)C(b7)C(b8)	107.17 (53)
FeN(3)C(a5)	126.89 (32)	C(a8)C(b8)C(b7)	108.09 (48)
FeN(3)C(a6)	127.80 (32)	C(a2)C(m1)C(a3)	122.76 (49)
C(a5)N(3)C(a6)	104.98 (40)	C(a4)C(m2)C(a5)	122.13 (46)
FeN(4)C(a7)	127.39 (34)	C(a6)C(m3)C(a7)	122.02 (46)
FeN(4)C(a8)	126.70 (36)	FeF(1)Sb	150.38 (24)
C(a7)N(4)C(a8)	105.88 (41)	F(1)SbF(2)	177.72 (17)
N(1)C(a1)C(b1)	109.21 (51)	F(1)SbF(3)	90.60 (20)
N(1)C(a1)C(m4)	126.34 (53)	F(1)SbF(4)	87.02 (24)
C(b1)C(a1)C(m4)	124.45 (52)	F(1)SbF(5)	87.77 (21)
N(1)C(a2)C(b2)	110.89 (50)	F(1)SbF(6)	91.01 (25)
N(1)C(a2)C(m1)	126.32 (50)	F(2)SbF(3)	91.34 (23)
C(b2)C(a2)C(m1)	122.74 (54)	F(2)SbF(4)	91.77 (31)
N(2)C(a3)C(b3)	110.83 (45)	F(2)SbF(5)	90.25 (24)
N(2)C(a3)C(m1)	125.12 (45)	F(2)SbF(6)	90.13 (32)
C(b3)C(a3)C(m1)	124.03 (47)	F(3)SbF(4)	90.57 (47)
N(2)C(a4)C(b4)	109.62 (48)	F(3)SbF(5)	177.63 (31)
N(2)C(a4)C(m2)	126.48 (45)	F(3)SbF(6)	91.51 (31)
C(b4)C(a4)C(m2)	123.79 (48)	F(4)SbF(5)	87.63 (38)
N(3)C(a5)C(b5)	109.81 (45)	F(4)SbF(6)	177.15 (40)
N(3)C(a5)C(m2)	126.81 (48)	F(5)SbF(6)	90.24 (42)
C(b5)C(a5)C(m2)	123.38 (49)		

[a] The numbers in parentheses are the estimated standard deviations.

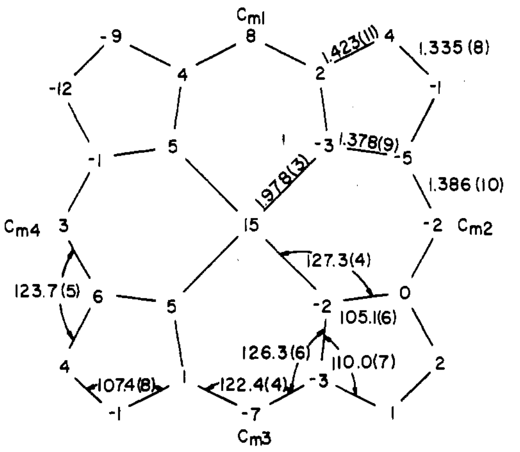

Figure 3. Formal diagram of the porphinato core displaying the perpendicular displacements, in units of 0.01 Å, of each atom from the mean plane of the 24-atom core. Average values for a number of bond parameters are also shown.

atom. This is also implied by the Fe–F distance of 2.105 (3) Å, which is much longer than that observed in either high-spin Fe(TPP)F[24] (1.792 (3) Å) or the 1.966 (2) Å Fe–F bond found in Fe(TPP)(F)$_2$.[30] It is also significantly larger than the Fe–F distances observed in a number of polymeric ferric fluorides.[31]

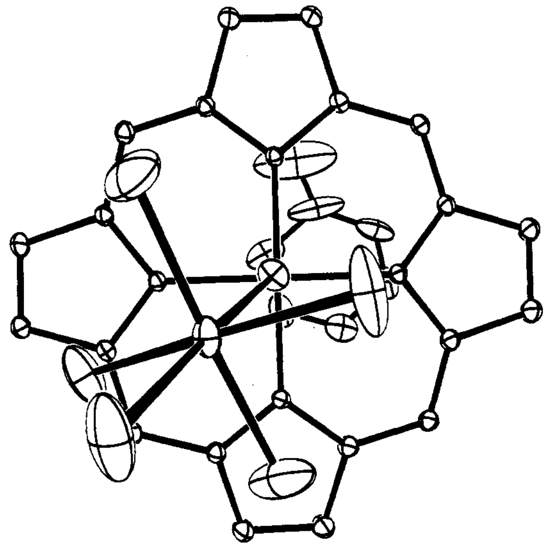

Figure 4. View of Fe(TPP)(FSbF$_5$)·C$_6$H$_5$F showing the orientation of the hexafluoroantimonate ligand and the disposition of the fluorobenzene solvate. The porphinato core is in the plane of the paper.

Individual bond distances and bond angles for Fe(TPP)(FSbF$_5$) are listed in Tables II and III, respectively. The numbering scheme used is shown in Figure 2. Also displayed in Figure 2 are the bond distances in the coordination group. Figure 3 displays the displacement (in units of 0.01 Å) of the atoms from the mean plane of the 24-atom core. The deviations from planarity of the core in Fe(TPP)(FSbF$_5$) are typical of the minor ruffling observed in many nearly planar metalloporphyrins. Figure 1 also displays the average values of bond distances and bond angles for the various classes in the porphinato core. The dihedral angles between the peripheral phenyl groups and the mean plane of the core are 59.4, 70.9, 78.0, and 78.8°; these are within the range of values usually observed.

The average Fe–N distance of 1.978 (3) Å and the small displacement of the iron atom out of the porphinato mean plane are in general accord with those expected[14] for an intermediate-spin state of predominant $S = {}^3/_2$ character and not for a high-spin state. The average Fe–N bond distance is in fact slightly shorter than those observed previously for admixed intermediate-spin iron(III) porphyrinate derivatives: 2.001 (5) Å in Fe(TPP)(OClO$_3$),[3] 1.994 (23) Å in Fe(OEP)(OClO$_3$),[6] 1.995 (3) Å in the polymer [Fe(TPP)(C(CN$_3$))]$_n$,[9] and 2.005 (6) Å in the monoclinic form of [Fe(OEP)(3-Cl-py)$_2$]$^+$.[12] This indication of increased tetragonality of the ligand field is consistent with the idea that the spin state of Fe(TPP)(FSbF$_5$) more nearly approaches a pure $S = {}^3/_2$ state.

The length of the M–N$_p$ bonds in five-coordinate metalloporphyrin derivatives is dependent on the size of the central hole (Ct···N) and the metal atom displacement. In the three structurally characterized five-coordinate admixed intermediate-spin iron(III) species, the hole sizes are essentially identical.[32] However, the iron atom displacement is much smaller in Fe(TPP)(FSbF$_5$).[33] Thus, the smaller average Fe–N bond distance in Fe(TPP)(FSbF$_5$) appears to be directly attributable to the smaller displacement of the iron atom from the central hole. Two possible factors might be responsible for this smaller displacement compared to the perchlorato derivatives. First, there is an electronic effect from the difference in ligand field strengths of the perchlorate and hexafluoroantimonate ligands. The dimensions about iron are consistent with the idea that SbF$_6^-$ is both a weaker

---

(30) Scheidt, W. R.; Lee, Y. J.; Tamai, S.; Hatano, K. *J. Am. Chem. Soc.* **1983**, *105*, 778–782.

(31) Von der Muhll, R.; Ravez, J. *Rev. Chim. Miner.* **1974**, *11*, 652–663. Von der Muhll, R.; Daut, F.; Ravez, J. *J. Solid State Chem.* **1973**, *8*, 206–212. Von der Muhll, R.; Anderson, S.; Glay, J. *Acta Crystallogr., Sect. B: Struct. Crystallogr. Cryst. Chem.* **1971**, *B27*, 2345–2353. Babel, D.; Wall, F.; Heher, G. *Z. Naturforsch., B: Anorg. Chem., Org. Chem.* **1974**, *29B*, 139–148. Hepworth, M. A.; Jack, K. H.; Peacock, R. D.; Westland, G. J. *Acta Crystallogr.* **1957**, *10*, 63–67.

(32) Ct···N is 1.974 Å in Fe(TPP)(FSbF$_5$), 1.981 Å in Fe(TPP)(OClO$_3$), and 1.977 Å in Fe(OEP)(OClO$_3$). The near-identity of Ct···N occurs despite significant differences in core conformations. Fe(TPP)(OClO$_3$) has an S_4 ruffled core; the other two species have essentially planar cores.

(33) Displacements of iron from the mean plane of the 24-atom core are 0.30 Å in Fe(TPP)(OClO$_3$), 0.26 Å in Fe(OEP)(OClO$_3$), and 0.15 Å in Fe(TPP)(FSbF$_5$). For Fe(TPP)(FSbF$_5$), the displacement from the mean plane of the four nitrogen atoms is 0.13 Å.

field ligand and a more weakly bound ligand than ClO_4^-. A weaker field axial ligand would lead to a more nearly pure $S = {}^{3}/_{2}$ spin state and the iron atom would be expected to have a smaller ionic radius than that having significant $S = {}^{5}/_{2}, {}^{3}/_{2}$ admixed character. Second, there is a complex formed between the $Fe(TPP)(FSbF_5)$ molecule and the fluorobenzene solvate that might affect the iron atom position.

This π complex is illustrated in Figure 4. In general terms, it is similar to those previously reported for Cr(TPP),[34] Zn(TPP),[35] and Mn(TPP)[36] with toluene molecules of solvation. In these three species, the closest atom–atom approach involves the metal and an "electron-rich" atom of the toluene solvate.[37] Thus the metal appears to act as an acceptor. A second common feature of these structures is a bonded pair of toluene carbon atoms astraddle a pyrrole nitrogen atom. Both features are also seen in $Fe(TPP)(FSbF_5)$ (Figure 4). The closest contact between the Fe atom and the ring is to the ortho carbon C(25) at 3.34 Å. The average separation between the porphinato plane and the fluorobenzene plane is 3.30 Å, and the dihedral angle between these two planes is 7.0°. The subtle effects that this "solvation" of the iron atom might have on its position or on its magnetic properties cannot be judged with certainty. It is likely, however, that it can influence both the axial and equatorial ligand fields to some small degree.[38] Since the interplanar separation of the fluorobenzene molecule in $Fe(TPP)(FSbF_5)\cdot C_6H_5F$ is smaller than analogous separations in the perchlorate structures, it is likely that any effects will be more pronounced in the present compound.

Conclusion

$Fe(TPP)(FSbF_5)$ is shown to have a coordinated hexafluoroantimonate ligand rather than an ionic structure, and the synthetic prospects for producing the truly unligated cation $[Fe(TPP)]^+$ do not look very promising. It remains a desirable goal, however, to synthesize some type of bare iron(III) porphyrin cation because such a species is expected to have a pure $S = {}^{3}/_{2}$ intermediate spin state. An example of an apparently pure intermediate-spin iron(III) porphyrin system showing no detectable admixture of an $S = {}^{5}/_{2}$ state is found in a vinylidene insertion compound.[39,40] A posible example in a system having a normal porphyrin ligand is suggested by the solution NMR properties of the 2,4,6-trimethoxy-substituted tetraphenylporphyrin iron(III) perchlorate system,[41] but the magnetic moment of 4.6 μ_B indicates there is probably some admixed $S = {}^{3}/_{2}, {}^{5}/_{2}$ character, at least in the solid state. In fact, the present compound, $Fe(TPP)(FSbF_5)\cdot C_6H_5F$, has a solid-state magnetic moment (4.14 μ_B) that more closely approaches the spin-only value of a pure $S = {}^{3}/_{2}$ state (3.90 μ_B) than any intermediate-spin iron(III) porphyrin so far reported. A detailed investigation of its electronic state is now under way with Mössbauer, magnetic, and EPR physical measurements, and this should determine whether there is any significant admixture of an $S = {}^{5}/_{2}$ state into its otherwise clearly demonstrated $S = {}^{3}/_{2}$ ground state.

Acknowledgment. This work was supported at the University of Southern California by the National Science Foundation (Grant No. CHE-8026812) and at the University of Notre Dame by the National Institutes of Health (Grant No. HL-15627).

Note Added in Proof. Coordinated hexafluoroantimonate has also been characterized recently by X-ray crystallography in $W(FSbF_5)(NO)(CO)(PPhMe_2)$: Hersh, W. H. *J. Am. Chem. Soc.* **1985**, *107*, 4599–4601.

Registry No. $[Fe(TPP)(FSbF_5)]\cdot C_6H_5F$, 98920-00-4; Fe(TPP)Br, 25482-27-3.

Supplementary Material Available: Table A (anisotropic temperature factors), Table B (fixed hydrogen atom positions), and a listing of structure factor amplitudes (×10) (24 pages). Ordering information is given on any current masthead page.

---

(34) Scheidt, W. R.; Reed, C. A. *Inorg. Chem.* **1978**, *17*, 710–714.

(35) Scheidt, W. R.; Kastner, M. E.; Hatano, K. *Inorg. Chem.* **1978**, *17*, 706–710.

(36) Kirner, J. F.; Reed, C. A.; Scheidt, W. R. *J. Am. Chem. Soc.* **1977**, *99*, 1093–1101.

(37) The M--C contacts are 3.36 (CrTPP), 3.12 (ZnTPP), and 3.05 Å (MnTPP). The carbon atom involved is either ortho or para to the toluene methyl substituent.

(38) The differences in solution NMR spectra of $Fe(TPP)(OClO_3)$ as a function of solvent suggest that there is some effect.[7]

(39) Mansuy, D.; Morgenstern-Badarau, I.; Lange, M.; Gans, P. *Inorg. Chem.* **1982**, *21*, 1427–1430.

(40) Olmstead, M. M.; Cheng, R.-J.; Balch, A. L. *Inorg. Chem.* **1982**, *21*, 4143–4148.

(41) Toney, G. E.; Terharr, L. W.; Savin, J. E.; Gold, A.; Hatfield, W. E.; Sangaish, R. *Inorg. Chem.* **1984**, *23*, 2563–2564.